

Trigonometric Parallax of the Protoplanetary Nebula OH 231.8+4.2

Y. K. Choi^{1*}, A. Brunthaler¹, K. M. Menten¹ and M. J. Reid²

¹Max-Planck-Institut für Radioastronomie, Auf dem Hügel 69, 53121 Bonn, Germany

*email: ykchoi@mpifr-bonn.mpg.de

²Harvard-Smithsonian Center for Astrophysics, 60 Garden Street, Cambridge, MA 02138, USA

Abstract. We report a trigonometric parallax measurement for the H₂O masers around the protoplanetary nebula OH 231.8+4.2 carried out with the Very Long Baseline Array (VLBA). Based on astrometric monitoring for 1 year, we measured a parallax of 0.65 ± 0.01 mas, corresponding to a distance of $1.54^{+0.02}_{-0.01}$ kpc. The spatial distribution of H₂O masers is consistent with that found in the previous studies. After removing the average proper motion of 1.4 mas yr⁻¹, corresponding to 10 km s⁻¹, the internal motions of the H₂O maser spots indicate a bipolar outflow.

Keywords. masers, astrometry, stars: late-type, stars: distances, stars: individual (OH 231.8+4.2)

1. Introduction

A protoplanetary nebula (PPN) is in a transition phase from an asymptotic giant branch (AGB) star to a planetary nebula (PN). Compared with the spherically symmetric circumstellar envelopes around AGB stars, PPNe and PNe show asymmetries, frequently clear bipolarity, and collimated winds. The evolution of post-AGB objects is still not well understood. Several models have postulated the presence of rings or disks close to the post-AGB stars. The accretion of material from such structures might create a post-AGB jet and the interaction between such a jet and the remnant AGB envelope produces shocks in the PPN lobes. Since H₂O and SiO masers probe the structure and kinematics of the inner nebular region, they are good tools to understand the formation of bipolar PPNe.

OH 231.8+4.2 is a well studied PPN, showing H₂O and SiO maser emission. The central source is a binary system, composed of an M9-10 III Mira variable (i.e. an AGB star) and an A0 main-sequence companion (Sánchez Contreras *et al.* 2004). This bipolar nebula shows signs of post-AGB evolution: fast bipolar outflows with velocities 200–400 km s⁻¹, shock-excited gas and shock-induced chemistry (Morris *et al.* 1987).

Previous VLBI phase referencing observations (Desmurs *et al.* 2007) successfully determined the absolute positions of the H₂O and SiO ($v = 2, J = 1 - 0$) masers. The H₂O maser clumps are detected in two regions separated by ~ 60 mas nearly in the north-south direction, suggestive of a bipolar outflow. The northern region has blue-shifted emission and the southern red-shifted emission, relative to the central star's velocity. The SiO masers, most likely indicating the position of the Mira component of the binary system, are located between the two H₂O maser regions. The distribution of the SiO masers in OH 231.8 is elongated perpendicular to the nebular axis, suggesting the presence of an equatorial torus or disk around the central star.

Measuring trigonometric parallaxes of PPNe is crucial for determining their fundamental properties of luminosity, mass-loss rate, age, and initial mass. Thanks to the VLBI technique, distance measurements via trigonometric parallaxes have become possible even

beyond several kpc. Here, we present the results from our multi-epoch phase-referencing VLBI observations of the H₂O masers toward OH231.8+4.2.

2. Observations

We have conducted Very Long Baseline Array (VLBA) observations to study the H₂O masers at a rest frequency of 22.235080 GHz toward the PPN OH 231.8+4.2. In order to measure a trigonometric parallax, we used phase-referencing observations by fast switching between the maser target and the extragalactic continuum source, J0746-1555, separated by 1.55 degrees from OH 231.8+4.2. The VLBA observations were scheduled under program BC188 at four epochs: 2009 May 01, Oct 19, Nov 09 and 2010 May 01. These dates were optimized to get the maximum and minimum of the parallax signal in right ascension.

We placed a strong source, J0530+1331, near the beginning, middle, and end of the observations to monitor delay and clock offsets. In order to calibrate atmospheric delays, we placed geodetic blocks before and after our phase-referencing observations (Reid *et al.* 2009).

The data were correlated in two passes with the VLBA correlator in Socorro, NM. The four dual-polarized frequency bands of 8 MHz bandwidth were processed with 16 spectral channels for each frequency band. The one (dual-polarized) frequency band containing maser emission was processed with 1024 channels, giving a velocity resolution of 0.10 km s⁻¹. The data reduction was performed with the NRAO AIPS package and ParselTongue scripts.

3. Results

3.1. Spatial distribution of maser spots

Fig. 1 (left) shows the 22 GHz H₂O maser spectrum toward OH231.8+4.2 on 2010 May 01 produced by scalar averaging the data over all times and baselines. The H₂O masers span LSR velocities ranging from 24 to 45 km s⁻¹. Though there are variations in the

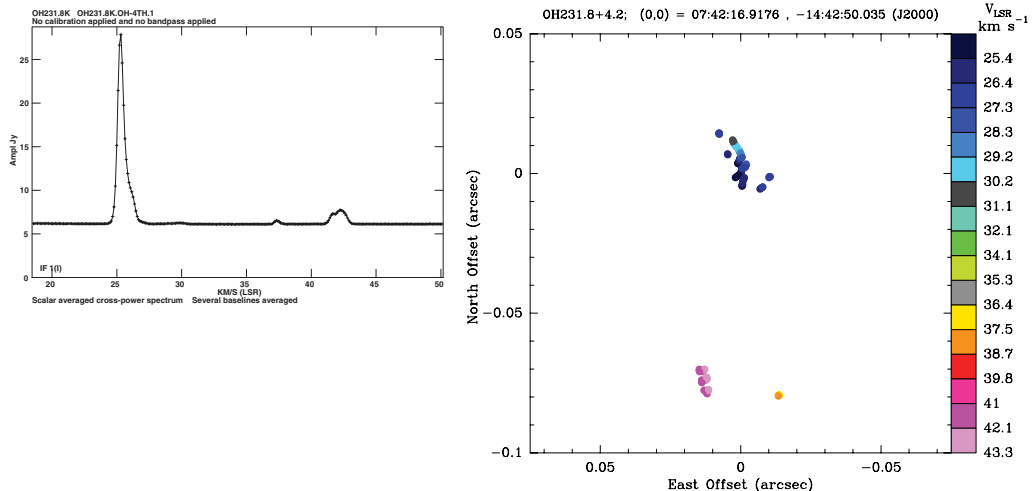


Figure 1. Spectrum and spatial distribution of the H₂O masers toward OH231.8+4.2. Left panel: the spectrum on 2010 May 01 produced by scalar averaging the data over all times and baselines. Right panel: the spatial distribution on 2010 May 01. The LSR velocity of the maser spots is indicated by the color bar to the right.

flux density, the overall structures of the maser spectrum are common to all epochs, indicating that the maser spots survive over the observing period of 1 year. We selected a stable and strong maser spot at an LSR velocity of 25.42 km s^{-1} as phase-reference.

The spatial distribution of H₂O masers toward OH231.8+4.2 relative to the reference maser spot at the LSR velocity of 25.42 km s^{-1} on 2010 May 01 is shown in the Fig. 1 (right). The H₂O maser spots are located within 40 mas in right ascension and 100 mas in declination. Compared with the previous study by Desmurs *et al.* (2007), the red-shifted components in south and the blue-shifted components in north indicate an outflow along the north-south direction.

3.2. Parallax measurements

Fig. 2 shows position measurements of the H₂O maser component at the LSR velocity of 25.42 km s^{-1} relative to the background continuum source J0746-1555 over 1 year. The position offsets are with respect to $\alpha(\text{J2000.0}) = 07^{\text{h}}42^{\text{m}}16^{\text{s}}9176$ and $\delta(\text{J2000.0}) = -14^{\circ}42'50''035$. Assuming that the movements of the maser features are composed of a linear motion and the annual parallax, we obtain a proper motion and an annual parallax by least-squares fitting. We measured the parallax of OH 231.8+4.2 to be 0.65 ± 0.01 mas, corresponding to a distance of $1.54^{+0.02}_{-0.01} \text{ kpc}$. This is the first high-accuracy distance that has been determined for OH 231.8+4.2. The absolute proper motion for this maser spot is $\mu_x = -4.35 \pm 0.02 \text{ mas yr}^{-1}$ toward the east and $\mu_y = 0.71 \pm 0.59 \text{ mas yr}^{-1}$ toward the north.

There are two more spots detected at all four epochs after phase-referencing. We estimated parallaxes and proper motions for those maser spots and list these in table 1. The results are consistent with each other. While the parallaxes should be identical within measurement uncertainties, the proper motions are expected to vary among the spots because of their internal motions.

3.3. Internal motion of maser spots

We also calculated the internal motions of the maser spots in right ascension and declination by a least-square fit for linear motion with respect to the reference spot. After

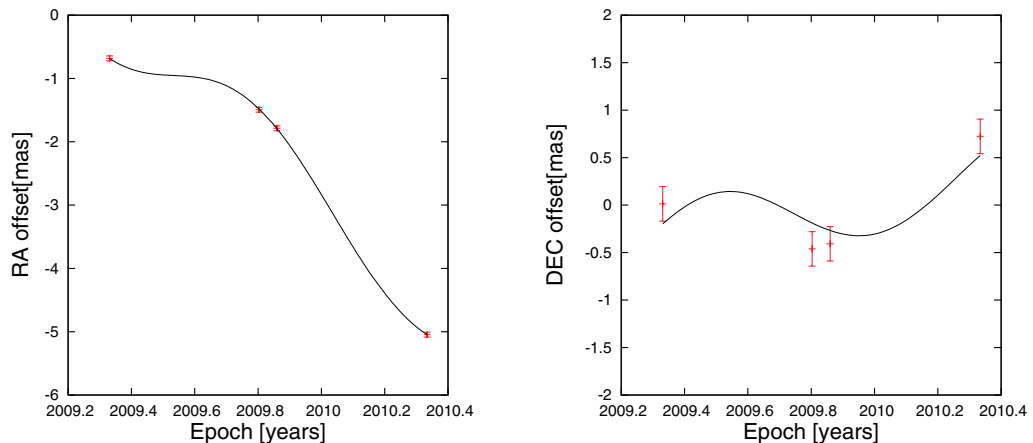


Figure 2. Parallax and proper motion data and fits for OH 231.8+4.2. Points with error bars are position measurements of the H₂O maser spot at an LSR velocity of 25.42 km s^{-1} relative to background quasar J0746-1555. Solid lines represent the best-fit model with an annual parallax and linear proper motions. Left panel: the change of position in right ascension as a function of time (year). Right panel: the same as the left panel in declination.

Table 1. Parallax and proper motions fits

LSR velocity (km s ⁻¹)	parallax (mas)	μ_x (mas yr ⁻¹)	μ_y (mas yr ⁻¹)
25.42	0.65 ± 0.01	-4.35 ± 0.02	0.71 ± 0.59
37.32	0.65 ± 0.02	-4.94 ± 0.07	-1.65 ± 0.02
41.85	0.66 ± 0.03	-4.05 ± 0.11	-1.75 ± 0.07
Combined	0.65 ± 0.01	-4.45 ± 0.14	-0.89 ± 0.45

removing the average relative motion of all maser spots of -0.136 mas yr⁻¹ eastward and -1.43 mas yr⁻¹ northward, the remaining internal motion vectors are shown in Fig. 3 and suggest a bipolar outflow. The blue-shifted components show an average motion of about 11 km s⁻¹ to the north, and the red-shifted components show an average motion of about 7–13 km s⁻¹ to the south for a distance of 1.5 kpc. Thus, the separation velocity between two components is about 20 km s⁻¹, which is consistent with the result reported by Leal-Ferreira *et al.* (2012).

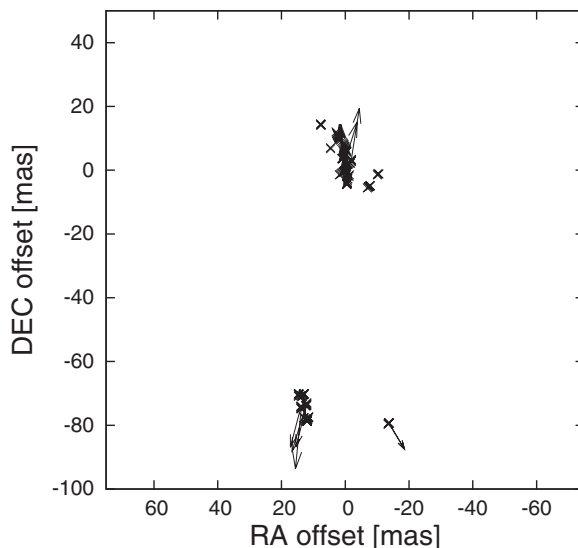


Figure 3. The internal motion of the H₂O maser spots toward OH 231.8+4.2 after removing the average relative motion with respect to the reference maser spot. Absolute coordinates of the map origin are α (J2000.0)=07^h42^m16^s9176 and δ (J2000.0)=−14°42'50''035.

Acknowledgements

This work has been supported by the ERC Advanced Grant GLOSTAR under grant agreement no. 247078.

References

- Desmurs *et al.* 2007, *A&A*, 468, 189
- Leal-Ferreira *et al.* 2012, *A&A*, 540, A42
- Morris *et al.* 1987, *ApJ*, 321, 888
- Reid *et al.* 2009, *ApJ*, 693, 397
- Sánchez Contreras *et al.* 2004, *ApJ*, 616, 519